2005-01-1203

A Parametric Study of Frictional Resistance to Vehicular Rotation Resulting from a Motor Vehicle Impact

Orion P. Keifer, Bradley C. Reckamp, Thomas C. Heilmann and Peter D. Layson
Applications Engineering Group, Inc.

ABSTRACT

The equations of rotational motion used to calculate pre-impact vehicle speeds using the rotational displacement of the vehicles following a collision are well known. The technique uses the rotational momentum exchange during impact and the principle of conservation of rotational energy to calculate the post impact vehicle angular velocity from the energy dissipated during the vehicle's rotation to a stop (product of torque and rotational displacement). Integral to the calculation of the stopping torque on the vehicle is the determination of the effective rotational coefficient of friction (f_r) between the tires and the roadway. The interactions of the road with the tires to produce the rotational coefficient of friction (f_r) are more complex and less understood than those of linear coefficient of friction (deceleration factor). A derivation of the post impact equations of motion and the kinematics of vehicles in rotation are examined. The resultant parameters of motion that affect the rotational coefficient of friction (f_r) are presented. The effects of these various parameters on the rotational coefficient of friction (f_r) were studied using EDSMAC™. Normalized coefficients, which can be multiplied by the roadway friction to obtain the rotational coefficient of friction (f_r) under common accident scenarios, are presented. Use of equations of rotational motion supplements linear momentum equations in a momentum analysis. They are not a substitute for other accident reconstruction techniques, such as computer crash simulations.

INTRODUCTION

A common problem faced in accident reconstruction is a lack of reliable information on which to base conservation of momentum calculations to determine pre-impact velocity. Occasionally, the only source of information regarding the final vehicle rest position is the un-scaled sketch included in a police report. When a reporting officer is attempting to sketch the scene and the final rest positions of the involved vehicles, he is frequently making no attempt to accurately establish positions or the distances between the point of impact and the final rest positions of the vehicles. Therefore, use of the sketch to estimate distances is problematic. The reporting officer is likely to be more accurate in the final rest angular orientation of the vehicles, especially with respect to scene features such as lane lines. As a result, the total vehicle rotational displacement information may, on a case to case basis, be more accurate and reliable than the available linear displacement information. Also problematic is the use of linear momentum equations in a collision between vehicles with a large mass mismatch, such as in a motorcycle-automobile impact. The linear displacement of the massive vehicle is small and the equations are very sensitive to slight inaccuracy of the measured distance. However, when significant rotation of the massive vehicle occurs, the rotational momentum equations can be far less sensitive.

While it is common practice to ignore post-impact rotational motion (and the energy associated with rotational velocity) the rotational displacement for each vehicle provides information for an additional equation to determine the impact velocity. This can be used to supplement the linear momentum equations when information is missing or questionable, or to act as a second check. It is significant to note that the rotational momentum equations are scalar, when considering planar motion, in contrast to the linear momentum equations which require both magnitude and direction (vector).

Analogous to linear momentum calculations, rotational momentum equations are based upon calculation of the energy dissipated while the vehicle rotates to a stop in order to find the post-impact angular velocity. Integral to this calculation is the force between the road surface and the tires that is retarding rotation. This force is normalized to the weight of the vehicle and is expressed as the rotational coefficient of friction (f_r), which produces the torque (moment) to stop the rotation of the vehicle.

The objective of this study is to determine the factors which affect the rotational coefficient of friction (f_r) and determine a baseline rotational coefficient of friction (f_r) for common situations. The data has been normalized and presented in graphical form for use by accident reconstruction professionals.

ROTATIONAL MOTION

The equations that describe linear and rotational momentum transfer in an offset vehicle collision have been published over many years (1, 2, 3) and expanded to compute impact speeds of both vehicles (4). The equations are used in the LARM2 accident reconstruction software (5). While most of the required input variables are post impact scene and vehicular data, the rotational coefficient of friction (f_r) is relegated to the judgment of the accident reconstruction professional. Current published values for the rotational coefficient of friction (f_r) give a range of 0.1 to 0.5 (5). An understanding of the derivation of the equation that uses (f_r), the factors that have a significant effect on (f_r) and a way to calculate (f_r), knowing the coefficient of friction of the road surface at the scene of the accident will be addressed.

POST-IMPACT KINETIC EQUATIONS

In linear momentum calculations, it is necessary to know the post impact velocity of the vehicles. The velocity is calculated from the following linear conservation of energy equation:

$$\frac{1}{2}mV^2 = Fd \quad \text{(Equation 1)}$$

where: m – mass of the vehicle
V – vehicle post impact velocity
F – force acting on the vehicle
d – distance over which the force acts

For the force, substitute in the following, representing the tire roadway interaction:

$$F = a_g mf \quad \text{(Equation 2)}$$

where: F – force acting on the vehicle
m – mass of the vehicle
a_g – acceleration of gravity
f – linear coefficient of friction (deceleration factor)

The equation now becomes:

$$\frac{1}{2}mV^2 = a_g mfd \quad \text{(Equation 3)}$$

which rearranged becomes:

$$V = \sqrt{2a_g fd} \quad \text{(Equation 4)}$$

This now relates the post impact velocity to the scene information (distance traveled) with an appropriately measured or assumed deceleration factor (f).

The rotational conservation of energy equations are analogous. The post-impact rotational energy is equal to the energy dissipated as the vehicle rotates to a stop as follows:

$$\frac{1}{2}I\omega^2 = T\theta \quad \text{(Equation 5)}$$

where: I – yaw mass moment of inertia of the vehicle
ω – vehicle post impact angular velocity
T – torque (moment) acting on the vehicle
θ – rotational displacement from impact to final rest

At this point, the derivations of published equations assume that the center of gravity of the vehicle is located half way between the front and rear axles and that the force at each wheel responsible for the stopping torque (moment) is collinear with the axle, that is the track width is neglected. The result is the moment arm for all wheels is half the wheel base length. The rotational coefficient of friction (f_r), a term used in previous work (Limpert 1989 and 1991), is the average lateral force developed to retard overall vehicle rotation, divided by the normal force on the wheels (weight of the vehicle). The force producing the moment is therefore the weight of the vehicle times the rotational coefficient of friction (f_r). The effective retarding torque produced to stop the rotation now becomes:

$$T = \frac{l_{wb}}{2} wf_r \quad \text{(Equation 6)}$$

where: T – torque (moment) acting on the vehicle
l_{wb} – wheel base length
w – weight of the vehicle
f_r – rotational coefficient of friction

Substituting for torque, in the conservation of energy equation becomes:

$$\frac{1}{2}I\omega^2 = \frac{l_{wb}}{2} wf_r\theta \quad \text{(Equation 7)}$$

Solving for the angular velocity, the equation becomes:

$$\omega = \sqrt{\frac{l_{wb}}{I} wf_r\theta} \quad \text{(Equation 8)}$$

For the purposes of this parametric study, the equation above was solved for the rotational coefficient of friction (f_r) as follows:

$$f_r = \frac{I\omega^2}{l_{wb}w\theta} = \frac{I}{l_{wb}w}\frac{\omega^2}{\theta} \quad \text{(Equation 9)}$$

Note that the $\frac{I}{l_{wb}w}$ term is comprised only of vehicle size related parameters. The second term $\frac{\omega^2}{\theta}$ only has variables describing the vehicle's kinematics. Therefore, for a given road surface, the rotational coefficient of friction (f_r) is a function of the vehicle's size/geometry and motion (the ratio of ω^2 to θ).

Several observations can be made from this derivation:

1. The rotational coefficient of friction (f_r) is dependent on the vehicle size parameters and is likely to change between various classes of vehicles.

2. Because it is assumed that the center of gravity is half way between the front and rear axles in the mathematical model, the calculated rotational coefficient of friction (f_r) may be different between a side impact to the front of the vehicle causing rotation and an identical side impact to the rear of the vehicle.

3. Because the force on all wheels is lumped into the rotational coefficient of friction (f_r), it is likely dependent upon braking, especially in cases where one wheel is locked because of impact damage.

POST IMPACT VEHICLE KINEMATICS WITH ROTATION

It is important to understand the motion of a rotating vehicle and the friction on the tires in order to understand the parameters that will affect the rotational coefficient of friction (f_r). If a model automobile is set on a flat surface and rotated about its center of gravity (rotation but no translation), a retarding force to the rotation will be developed due to the opposite direction of the side forces on the front and rear tires. Concomitantly, the wheels will turn, because the rolling planes of the wheels are offset from the centerline. Now visualize a moving vehicle which is rotating slowly with respect to its linear velocity. As it is sliding broadside, the frictional forces on both the front and rear wheels are acting in the same direction to retard the linear velocity and no net torque is developed to retard the rotational motion. While it is somewhat beyond the scope of this paper and examined elsewhere (6), at a velocity ratio between linear velocity (in feet or meters per second) and rotational velocity (in radians per second), of approximately one half the wheel base (in feet or meters), the tire forces simultaneously retard the linear motion and rotational motion. The resultant motion at this ratio is when the vehicle essentially spins about the center of one axle and then flips to spin about the center of its other axle, etc. If the velocity ratio is too small (too much rotational velocity), the tire forces preferentially slow the rotation, as in the spinning model discussed above. If the velocity ratio is too large (too much linear velocity) the tire forces preferentially slow the linear motion as discussed in the slowly rotating vehicle above. From the above discussion, several observations can be made.

1. The rotational coefficient of friction (f_r) is dependent on the coefficient of friction between the tires and the roadway (skidding drag coefficient).

2. The rotational coefficient of friction (f_r), for all practical purposes, will always be less than the coefficient of friction between the tires and the roadway.

3. The rotational coefficient of friction (f_r) is dependent upon the pre-impact velocity of the rotating vehicle that is being modeled.

4. The incremental torque (moment) on the vehicle is dependent on the instantaneous angle of the vehicle with respect to the direction of linear motion. Because rotational coefficient of friction (f_r) is an average over all of these incremental torques, the rotational coefficient of friction (f_r) will also be dependent upon the total rotational displacement at final rest.

PARAMETRIC STUDY USING EDSMAC™

EDSMAC™ (Version 2.51) was selected to perform this parametric study. This program has several advantages which make it well suited for use in this study. Vehicle characteristics are easily changed and the program takes into account tire characteristics in the calculated motion. Further, the results include the information to determine the total rotation of the vehicles from impact to final rest (θ) and the post impact angular velocity (ω), the two parameters needed to calculate the rotational coefficient of friction (f_r). Finally, EDSMAC™ is well documented and validated (7).

The parametric study of the rotational coefficient of friction (f_r) was conducted by simulating a target vehicle being struck perpendicularly near an axle by a bullet vehicle. This configuration is consistent with side impacts with significant target vehicle rotation, conditions for which this technique is most suited (Limpert, 1991). The speed of the bullet vehicle was adjusted to produce a desired total rotation from impact to final rest. The EDSMAC™ output included the initial angle, angle at final rest and angular velocity at separation for the target vehicle, which was then used to calculate f_r, as follows:

$$f_r = \frac{I}{l_{wb}w}\frac{\omega^2}{\theta} \quad \text{(Equation 10)}$$

Of note, EDSMAC™ also documents the angle of the vehicle at separation; however, the initial angle and final rest angle were used in this study to calculate the total rotational angle (θ). While arguably the angle at separation should be used because the angular velocity at separation was used, it is customary in accident reconstruction to assume the impact duration and motion during the impact is negligible. From a practical standpoint, the accident reconstructionist can only determine or estimate the initial angle and compare it to the final rest angle to determine rotational displacement for use in the derived equations.

The vehicle parameters for the bullet vehicle for all runs correspond to a 1998 Ford Expedition.

The initial work was to evaluate the effect of vehicle size, and roadway friction as a function of rotational displacement. Vehicle dimensional and inertial data, as listed in EXPERT AUTOSTATS®, were used for 3 target vehicles; a 1998 Geo Metro representing a small vehicle, a 1998 Honda Accord 4-door representing a medium vehicle, and a 1998 Ford Expedition representing a large vehicle. The impact scenario involved a stationary target vehicle with no braking, struck perpendicularly at the right rear wheel area by a bullet vehicle.

Data to calculate the rotational coefficient of friction (f_r) was taken for rotation angles of 15, 45, 90 120, 135, 150, 180, 210, 225, 240, 270, 300, 315, 330 and 360 degrees. A data run was considered acceptable if the total rotation was within 5 degrees of that targeted and in the case of the 15 degree measurement, a minimum of 15 degrees was required. This series of simulations was repeated using four road surface coefficients of friction (0.25, 0.5, 0.75 and 1.0). The process was repeated for each of the three target vehicles. The complete data is included in tabular form in Appendix A.

Additional simulations were conducted to examine the sensitivity of the rotational coefficient of friction (f_r) to other parameters, as follows:

1. Pre-impact target vehicle speeds of 5, 10, 15, 20, 25, and 30 miles per hour.

2. One wheel locked, corresponding to the point of impact on the target vehicle.

3. All four wheels of the target vehicle locked.

4. Target vehicle reversed so that the impact was to the right front wheel area of the target vehicle.

A roadway friction of 0.75 was used for all of the sensitivity simulations. Parameters for the 1998 Honda Accord were used for all four situations above. Additionally, simulations using the parameters for the 1998 Ford Explorer were conducted for situation 4, vehicle reversed. The complete data for these additional simulations is included in Appendix B.

RESULTS OF PARAMETRIC STUDY

As expected, the rotational coefficient of friction (f_r) was strongly affected by the roadway coefficient of friction. It was hypothesized that the relationship was linear. Therefore, a normalized rotational friction factor (ξ) was defined as follows:

$$\xi = \frac{f_r}{f} \quad \text{(Equation 11)}$$

Therefore, f_r can be calculated as follows:

$$f_r = \xi \cdot f \quad \text{(Equation 12)}$$

where: ξ – normalized rotational friction factor
f_r – rotational coefficient of friction
f – roadway skidding coefficient of friction

Figures 1 though 3 graphically show the normalized rotational friction factor (ξ) as a function of target vehicle rotational displacement for each of the three classes of vehicles (large medium, and small), respectively. Note, the four data points at each angle correspond to the four roadway coefficients of friction.

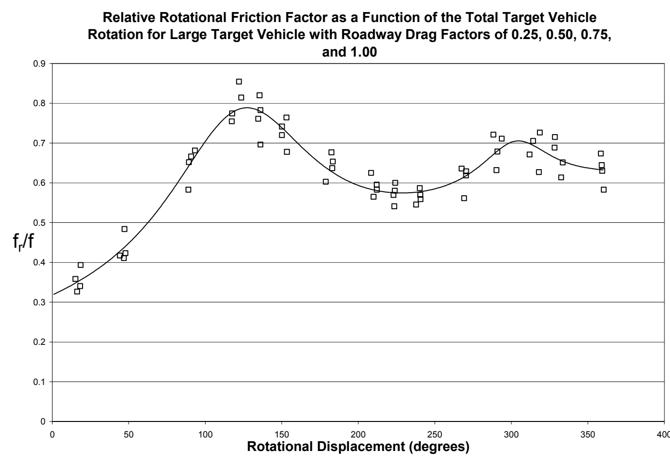

Figure 1

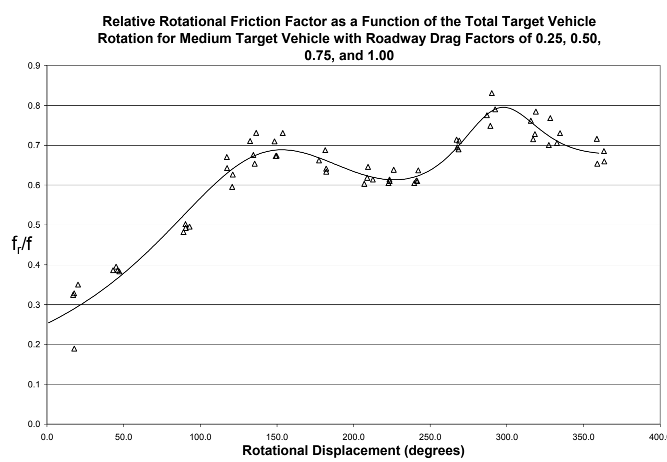

Figure 2

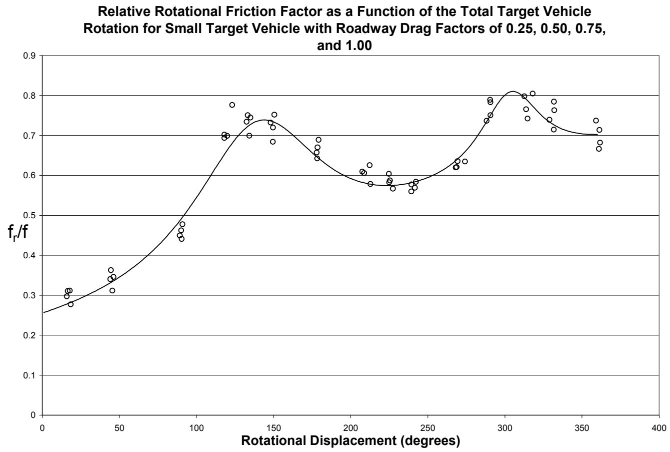

Figure 3

Because the points correspond reasonably well, all data is presented as the normalized rotational friction factor as a function of rotational displacement. A curve fit line for each vehicle (r = 0.96 for the large vehicle, r = 0.97 for the medium vehicle, and r = 0.98 for the small vehicle) is shown, with the mathematical function located in Appendix C.

Figure 4 graphically shows the normalized rotational friction factor as a function of target rotational displacement for all three vehicles and all four roadway coefficients of friction. A curve fit line for all vehicle and roadway friction data (r = 0.93) is also shown, with the mathematical function located in Appendix C.

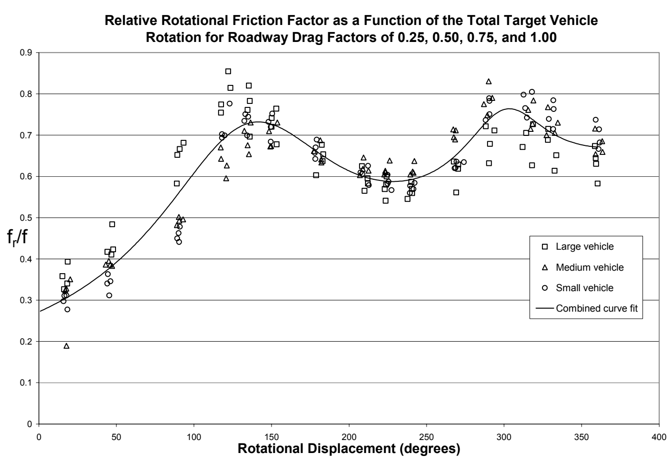

Figure 4

Figure 5 graphically shows the data for the medium target vehicle (1998 Honda Accord) traveling at 5, 10 15, 20, 25, and 30 miles per hour at impact. Note the curve fit line generated in figure 2, medium target vehicle (1998 Honda Accord), is shown for comparison.

Figure 6 graphically shows the data for the medium target vehicle (1998 Honda Accord) with all four wheels locked and with the struck wheel locked to simulate a locked wheel due to crush damage at impact. Note the curve fit line generated in figure 2, medium target vehicle (1998 Honda Accord), is shown for comparison.

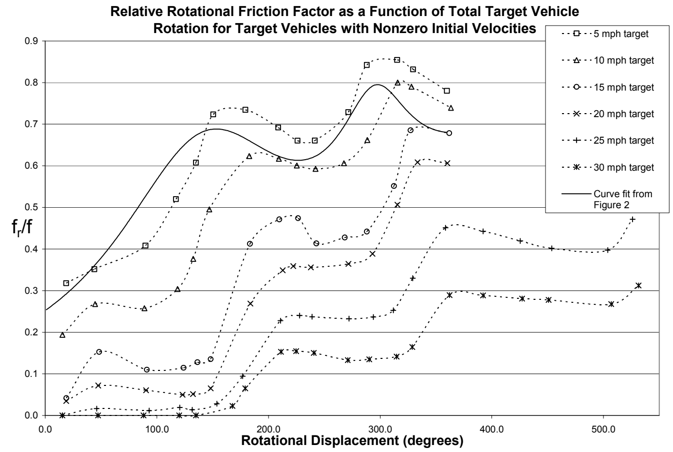

Figure 5

Figures 7 and 8 graphically show the data for the medium (1998 Honda Accord) target vehicle and large (1998 Ford Expedition) target vehicle, with the impact configuration changed to provide impact to the right front wheel instead of the right rear wheel of the target vehicle. Note the curve fit lines generated in figure 2, medium target vehicle (1998 Honda Accord), and figure 1, large target vehicle (1998 Ford Expedition), respectively, are shown for comparison.

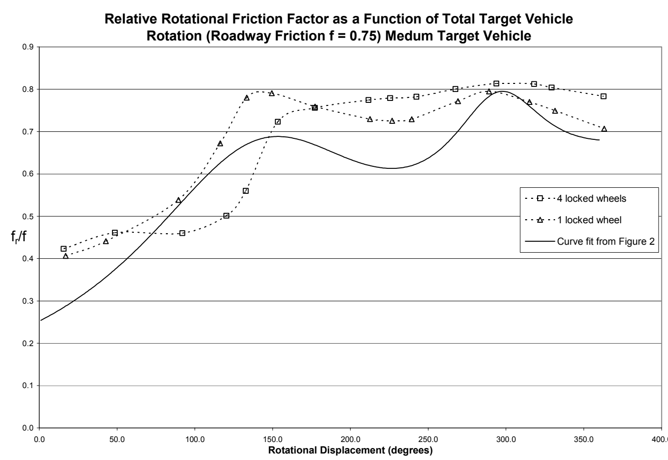

Figure 6

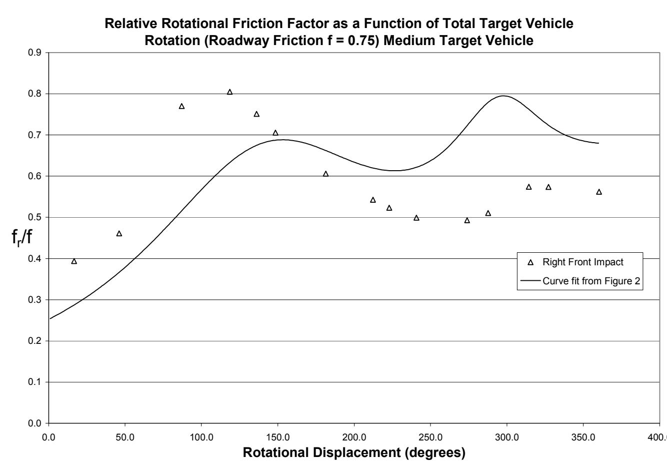

Figure 7

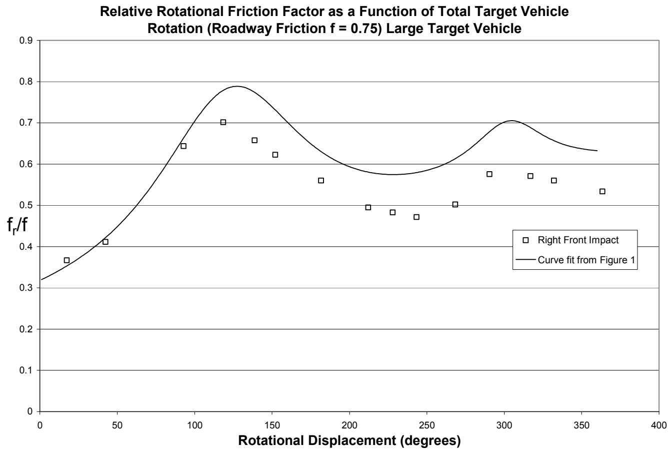

Figure 8

DISCUSSION AND ANALISYS

Figures 1 through 4 (see Appendix D for larger figures) show that over the range of 0 to 360 degrees of rotational displacement, the normalized rotational friction factor is bimodal, with peaks at rotational displacement angles of approximately 140 and 300 degrees. From a kinetic standpoint, the impact scenario causes the linear velocity at the center of gravity of the vehicle to be in the direction of the principal direction of force, which is perpendicular to the vehicle's axis. Higher torque is apparently experienced by the vehicle at displacement angles near 90 and 270 degrees, where the vehicle axis is aligned with the linear motion. At these angles, the wheels are rolling in the direction of linear motion and the side force on the tires is dedicated to stopping the rotation with opposite forces on the front and rear wheels. The peaks at 140 and 300 degrees of rotational displacement represent angles at which the vehicle has just completed this high torque portion of the rotational sequence and is entering a region of lower instantaneous torque. This phenomenon manifested itself during the parametric testing in that the portion of the curve between the peaks at approximately 140 and 300 degrees to the next relative minimum was very sensitive to the speed of impact of the bullet vehicle and the data was difficult to obtain within the specified 5 degree limit of acceptability. This is predictable from the following equation of rotational motion (equation 8):

$$\omega = \sqrt{\frac{l_{wb}}{I} w f_r \theta}$$

In this portion of the curve, the rotational coefficient of friction (f_r) is decreasing as the rotational displacement (θ) is increasing. The two terms counteract each other and the angular velocity (ω), which is a direct function of the impact velocity of the bullet vehicle, doesn't change much over this rotational displacement range. Consequently, slight changes in the bullet vehicle velocity cause significant changes in the resultant rotational displacement of the target vehicle. It further follows that since this range of rotational displacement values is produced by a narrow range of impact velocities, the probability of finding a target vehicle within this range of rotational displacement is small compared to other portions of the curve.

Figure 4 (see Appendix D) includes data for all three target vehicle sizes and all four roadway friction values. Remarkably, data correlates reasonably well at least in the range of vehicle sizes between the Ford Expedition and the Geo Metro. Vehicle size appears to have a modest effect on the rotational coefficient of friction (f_r). Also note that the curve appears to be a damped sinusoid that settles out at approximately 70% of the available roadway friction (ξ = 0.7). Assuming that the force causing the torque is sinusoidal from full value of roadway friction to negative full value of roadway friction, the root mean square of the frictional force causing the torque would be approximately 0.707 times the roadway friction. While hardly a proof, it appears that use of a normalized rotational friction factor, of approximately 70% of the available roadway friction (ξ = 0.7) for very large angles of rotational displacement (greater than approximately 300 degrees) is reasonable.

Figure 5 (see Appendix D) graphically demonstrates the effect of target vehicle speed on the rotational coefficient of friction. As discussed in the kinematics section, when the linear velocity is relatively high with respect to the angular velocity, the tire friction will preferentially retard the linear velocity with less effect on the angular velocity. This is clearly visible at the higher values of pre-impact target velocity. Remarkably, for target vehicle speeds of 20 miles per hour or less, there does seem to be a rotational displacement angle above which the curves approach the curves for the target vehicles that are stopped pre-impact (figure 4). Also of note, the peaks appear to be shifted to the right toward larger displacement angles as the pre-impact target velocity is increased. This is also predictable. The linear motion of the vehicle's center of gravity is the vector sum of the initial velocity of the target vehicle and the perpendicular velocity imparted during the impact. It therefore takes a greater angle of rotation of the vehicle to be aligned axially with the direction of the linear velocity. The 30 miles per hour initial target velocity curve, and to a lesser extent the 25 miles per hour curve, show a low normalized rotational coefficient of friction (ξ) even at 360 degrees of rotational displacement. Therefore, the testing was extended beyond a full revolution of rotational displacement. Because the normalized rotational coefficient of friction (ξ) is significantly smaller in this case for all ranges of rotational displacement, variations from vehicle to vehicle and roadway friction may have a more significant effect on the results of the calculations of pre-impact velocity with larger pre-impact target velocity. Therefore, great care must be taken by the accident reconstructionist to ensure that resultant calculations are supported by the actual accident conditions and case evidence.

Figure 6 (see Appendix D) shows the effect of locked wheels (braking forces). As expected the sinusoidal effect is reduced for one locked wheel and in the case of all four wheels being locked (full braking), it is essentially eliminated. It is also noteworthy that the normalized rotational friction factor never reaches a value of 1.0. That supports that the rotational friction factor (f_r) is always less than the roadway friction available, as predicted.

Figure 7 (see Appendix D) shows the effect of the impact to the right front wheel instead of the right rear wheel for the medium (1998 Honda Accord) target vehicle. You will note that the first peak is somewhat greater in magnitude and the second peak somewhat less in magnitude than for the medium target vehicle that was impacted on the right rear (figure 2). This difference is believed to be due to the variation of weight on the front tires as opposed to the rear in the real world vehicle and is an artifact of the assumption that the moment arm is half way between the front and rear axles in the calculational model. Nonetheless, the trend is similar to the remainder of the data.

Figure 8 (see Appendix D) shows the effect of the impact to the right front wheel instead of the right rear wheel for the large (1998 Ford Expedition) target vehicle. The normalized rotational coefficient of friction is lower throughout the range of rotational displacements. While it is likely that much of this difference is due to the variation of weight on the front tires as opposed to the rear in a real world vehicle, the larger ratio of the mass moment of inertia to mass must also have an effect.

CONCLUSION

1. The use of equations of rotational motion can supplement linear momentum equations in a momentum analysis. They are not a substitute for other accident reconstruction techniques, such as computer crash simulations.

2. The above data are generated with a target vehicle being struck perpendicularly near an axle by a bullet vehicle. This configuration is consistent with side impacts with significant target vehicle rotation, conditions for which rotational momentum analysis is best suited.

3. The rotational coefficient of friction (f_r) can be found by multiplying the appropriate normalized rotational friction factor (ξ), selected from the figures, by the roadway coefficient of friction (f), equation 12.

4. For slow moving (less than 10 miles per hour) target vehicles without braking, regardless of a front or rear lateral impact, figure 4 gives reasonable values for normalized rotational friction factor (ξ).

5. Use of figures 5 and 6 will assist the accident reconstructionist in assigning values for the rotational coefficient of friction (f_r) under conditions that the target vehicle has significant pre-impact velocity or is braking.

6. These data are not a substitute for sound judgment on the part of the accident reconstructionist when considering a specific case; however, insight into the vehicle kinematics and kinetics during rotation, as well as trends and magnitude of the rotational coefficient of friction (f_r) in the specific scenarios studied here should benefit the accident reconstructionist in assigning appropriate values for f_r.

REGISTERED TRADEMARKS

ACKNOWLEDGMENTS

The authors would like to extend special thanks to Richard V. Conte and Jacob Scott for their astute critique and assistance in this work.

REFERENCES

1. Boehm, R., and Hoerz, E., The Off-Center Impact of Two Pneumatic-Tired Vehicles, Autmobiltechnische Zeitschrift 70 (11), pp 385-389, 1968.
2. Buschmann and Koessler, Motorvehicle Handbook, Vol. 1, Wilhelm Heyne Publischer, Munich, Germany, 1976.
3. Limpert, Rudolf, Motor Vehicle Accident Reconstruction and Cause Analysis, 3rd Edition, Michie Company, Charlottesville, Virginia, 1989.
4. Limpert, Rudolf and Andrews, Dennis, Linear and Rotational Momentum for Computing Impact Speeds in Two-Car Collisions (LARM), SAE 910123, Society of Automotive Engineers, Warrendale, Pennsylvania, 1991.
5. LARM2 Reference Manual, ProSource Software, Provo, Utah, 1994.
6. Keifer, Orion P, Conte, Richard V., and Reckamp, Bradley C., Rotational and Linear Motion Analysis in Accident Reconstruction, In preparation.
7. Day, T.D., Hargens, R.L., Further Validation of EDSMAC™ using RICSAC Staged Collisions, SAE 900102, Society of Automotive Engineers, Warrendale, Pennsylvania, 1990.

CONTACT

Orion P. Keifer, P.E., Principal Mechanical Engineer
Bradley C. Reckamp, P.E., Senior Mechanical Engineer
Thomas C. Heilmann, Principal Scientist
Peter D. Layson, Principal Staff Scientist
Applications Engineering Group, Inc.
1200 Mayport Road, Atlantic Beach, Florida 32233
(800) 777-7668
aegi@aegiforensics.com

SYMBOLS

a_g – acceleration of gravity

d – distance over which the force acts

f_r – rotational coefficient of friction

f – roadway coefficient of friction

F – force acting on the vehicle

I – yaw mass moment of inertia of the vehicle

l_{wb} – wheel base length

m – mass of the vehicle

r – correlation coefficient

w – weight of the vehicle

V – vehicle post impact velocity

θ – rotational displacement from impact to final rest

T – moment (torque) acting on the vehicle

ξ – normalized rotational friction factor

ω – vehicle post impact rotational velocity

APPENDIX A

Large Vehicle (1998 Ford Expedition): Yaw Moment of Inertia = 3841 lb-ft-sec^2 - Weight = 4900 lb - Wheelbase = 119 in

Roadway Friction Factor, f	Rotational Velocity at Separation, ω (°/sec)	Total Rotational Displacement, θ (°)	Rotational Friction Factor, f_r	Normalized Friction Factor, ξ
1	62.1	16.3	0.33	0.33
1	118.0	46.8	0.41	0.41
1	193.9	89.0	0.58	0.58
1	253.4	117.4	0.75	0.75
1	262.1	136.1	0.70	0.70
1	274.5	153.4	0.68	0.68
1	279.5	178.8	0.60	0.60
1	293.3	210.0	0.57	0.57
1	296.1	223.6	0.54	0.54
1	306.6	237.8	0.55	0.55
1	330.9	269.2	0.56	0.56
1	364.7	290.3	0.63	0.63
1	380.2	318.1	0.63	0.63
1	384.6	332.6	0.61	0.61
1	390.2	360.4	0.58	0.58
0.75	54.4	15.2	0.27	0.36
0.75	100.1	44.2	0.31	0.42
0.75	177.9	89.3	0.49	0.65
0.75	222.5	117.6	0.58	0.77
0.75	236.0	134.6	0.57	0.76
0.75	242.4	150.1	0.54	0.72
0.75	251.7	183.0	0.48	0.64
0.75	259.3	212.2	0.44	0.58
0.75	262.8	223.1	0.43	0.57
0.75	270.5	240.7	0.42	0.56
0.75	304.1	270.5	0.47	0.63
0.75	327.6	290.9	0.51	0.68
0.75	337.4	312.0	0.50	0.67
0.75	343.7	333.7	0.49	0.65
0.75	350.9	359.4	0.47	0.63
0.5	51.5	18.6	0.20	0.39
0.5	85.7	47.9	0.21	0.42
0.5	151.8	93.3	0.34	0.68
0.5	191.0	123.6	0.41	0.81
0.5	196.5	136.1	0.39	0.78
0.5	200.9	150.2	0.37	0.74
0.5	208.4	183.4	0.33	0.65
0.5	213.9	212.0	0.30	0.60
0.5	217.0	223.9	0.29	0.58
0.5	222.9	240.6	0.28	0.57
0.5	246.2	270.4	0.31	0.62
0.5	275.2	293.8	0.36	0.71
0.5	283.4	314.3	0.35	0.71
0.5	286.2	328.3	0.34	0.69
0.5	289.6	359.1	0.32	0.64
0.25	33.6	18.3	0.09	0.34
0.25	64.4	47.3	0.12	0.48
0.25	104.7	90.8	0.17	0.67
0.25	137.5	122.1	0.21	0.85
0.25	141.9	135.5	0.20	0.82
0.25	145.6	153.1	0.19	0.76
0.25	149.6	182.5	0.17	0.68
0.25	153.6	208.4	0.16	0.62
0.25	156.1	224.2	0.15	0.60
0.25	159.8	240.2	0.15	0.59
0.25	175.6	267.6	0.16	0.64
0.25	194.1	288.3	0.18	0.72
0.25	204.8	318.7	0.18	0.73
0.25	206.3	328.5	0.18	0.71
0.25	209.2	358.6	0.17	0.67

Medium Vehicle (1998 Honda Accord): Yaw Moment of Inertia = 1807 lb-ft-sec^2 - Weight = 2925 lb - Wheelbase = 107 in

Roadway Friction Factor, f	Rotational Velocity at Separation, ω (°/sec)	Total Rotational Displacement, θ (°)	Rotational Friction Factor, f_r	Normalized Friction Factor, ξ
1	69.3	17.7	0.33	0.33
1	122.3	47.2	0.38	0.38
1	195.3	93.0	0.50	0.50
1	243.9	120.8	0.60	0.60
1	270.7	135.5	0.65	0.65
1	288.9	149.8	0.67	0.67
1	309.0	182.2	0.63	0.63
1	321.3	207.0	0.60	0.60
1	333.7	222.7	0.60	0.60
1	346.1	239.6	0.60	0.60
1	397.8	268.9	0.71	0.71
1	423.1	289.2	0.75	0.75
1	433.0	317.1	0.71	0.71
1	435.4	327.4	0.70	0.70
1	440.6	359.0	0.65	0.65
0.75	58.5	17.0	0.24	0.32
0.75	101.6	43.1	0.29	0.39
0.75	166.3	90.5	0.37	0.49
0.75	217.0	121.2	0.47	0.63
0.75	237.5	134.6	0.51	0.68
0.75	249.5	149.2	0.50	0.67
0.75	269.1	182.1	0.48	0.64
0.75	284.5	212.6	0.46	0.61
0.75	290.8	223.5	0.46	0.61
0.75	302.4	241.0	0.46	0.61
0.75	339.6	267.6	0.52	0.69
0.75	371.4	287.0	0.58	0.77
0.75	379.0	318.3	0.55	0.73
0.75	381.5	332.7	0.53	0.71
0.75	385.6	363.5	0.49	0.66
0.5	54.1	20.2	0.18	0.35
0.5	85.7	46.0	0.19	0.39
0.5	133.2	89.0	0.24	0.48
0.5	176.7	117.5	0.32	0.64
0.5	197.3	132.5	0.36	0.71
0.5	208.7	148.4	0.35	0.71
0.5	220.3	177.4	0.33	0.66
0.5	231.1	208.9	0.31	0.62
0.5	238.1	223.4	0.31	0.61
0.5	246.7	241.6	0.30	0.61
0.5	276.6	268.4	0.34	0.69
0.5	309.1	292.4	0.40	0.79
0.5	315.2	315.6	0.38	0.76
0.5	317.9	334.7	0.37	0.73
0.5	320.8	363.3	0.34	0.69
0.25	26.4	17.8	0.05	0.19
0.25	60.7	45.1	0.10	0.40
0.25	96.8	90.3	0.13	0.50
0.25	127.5	117.3	0.17	0.67
0.25	143.6	136.5	0.18	0.73
0.25	152.4	153.8	0.18	0.73
0.25	160.6	181.5	0.17	0.69
0.25	167.2	209.4	0.16	0.65
0.25	172.8	226.2	0.16	0.64
0.25	178.6	242.2	0.16	0.64
0.25	198.6	267.2	0.18	0.71
0.25	223.2	290.1	0.21	0.83
0.25	227.4	318.9	0.20	0.78
0.25	228.3	328.3	0.19	0.77
0.25	230.4	358.7	0.18	0.72

Small Vehicle (1998 Geo Metro): Yaw Moment of Inertia = 656 lb-ft-sec^2 -- Weight = 1808 lb -- Wheelbase = 93 in

Roadway Friction Factor, f	Rotational Velocity at Separation, ω (°/sec)	Total Rotational Displacement, θ (°)	Rotational Friction Factor, f_r	Normalized Friction Factor, ξ
1	76.1	15.9	0.30	0.30
1	131.6	45.4	0.31	0.31
1	220.9	90.4	0.44	0.44
1	320.3	119.9	0.70	0.70
1	339.0	134.3	0.70	0.70
1	353.8	149.5	0.68	0.68
1	374.4	178.3	0.64	0.64
1	388.2	212.8	0.58	0.58
1	397.2	227.4	0.57	0.57
1	404.9	239.3	0.56	0.56
1	451.0	268.1	0.62	0.62
1	516.7	290.6	0.75	0.75
1	534.7	314.7	0.74	0.74
1	538.6	331.7	0.71	0.71
1	542.6	361.0	0.67	0.67
0.75	68.6	16.5	0.23	0.31
0.75	117.4	44.1	0.26	0.34
0.75	191.9	89.2	0.34	0.45
0.75	274.2	118.1	0.52	0.69
0.75	303.8	135.0	0.56	0.74
0.75	314.4	149.6	0.54	0.72
0.75	327.7	178.0	0.49	0.66
0.75	340.7	208.7	0.45	0.61
0.75	346.8	224.9	0.44	0.58
0.75	355.3	241.6	0.43	0.57
0.75	396.4	269.3	0.48	0.64
0.75	457.0	290.6	0.59	0.78
0.75	469.5	313.7	0.57	0.77
0.75	472.4	328.9	0.55	0.74
0.75	475.9	361.7	0.51	0.68
0.5	55.9	18.4	0.14	0.28
0.5	98.9	46.2	0.17	0.35
0.5	159.7	90.1	0.23	0.46
0.5	225.3	118.1	0.35	0.70
0.5	244.0	132.5	0.37	0.73
0.5	257.6	148.1	0.37	0.73
0.5	270.6	178.5	0.34	0.67
0.5	278.2	207.5	0.30	0.61
0.5	284.7	225.5	0.29	0.59
0.5	290.8	239.4	0.29	0.58
0.5	319.5	268.7	0.31	0.62
0.5	374.5	290.4	0.39	0.79
0.5	390.7	312.6	0.40	0.80
0.5	393.8	332.0	0.38	0.76
0.5	397.3	361.3	0.36	0.71
0.25	41.2	17.8	0.08	0.31
0.25	70.3	44.5	0.09	0.36
0.25	115.3	90.9	0.12	0.48
0.25	171.0	123.1	0.19	0.78
0.25	174.9	133.2	0.19	0.75
0.25	186.1	150.5	0.19	0.75
0.25	194.4	179.2	0.17	0.69
0.25	201.6	212.3	0.16	0.63
0.25	203.8	224.8	0.15	0.60
0.25	208.1	242.3	0.15	0.58
0.25	230.7	274.1	0.16	0.63
0.25	254.8	288.1	0.18	0.74
0.25	279.8	318.0	0.20	0.80
0.25	282.2	331.8	0.20	0.78
0.25	284.6	359.1	0.18	0.74

APPENDIX B

Medium Vehicle (1998 Honda Accord): Roadway Friction Factor, f = 0.75

Specialized Test Feature	Rotational Velocity at Separation, ω (°/sec)	Total Rotational Displacement, θ (°)	Rotational Friction Factor, f_r	Normalized Friction Factor, ξ
5 mph Target Vehicle	57.0	18.8	0.24	0.32
5 mph Target Vehicle	91.8	44.1	0.26	0.35
5 mph Target Vehicle	141.2	89.8	0.31	0.41
5 mph Target Vehicle	182.0	117.2	0.39	0.52
5 mph Target Vehicle	211.2	135.0	0.46	0.61
5 mph Target Vehicle	243.3	150.5	0.54	0.72
5 mph Target Vehicle	267.6	179.3	0.55	0.73
5 mph Target Vehicle	280.2	208.7	0.52	0.69
5 mph Target Vehicle	284.9	226.1	0.50	0.66
5 mph Target Vehicle	294.5	241.5	0.50	0.66
5 mph Target Vehicle	328.0	271.5	0.55	0.73
5 mph Target Vehicle	363.2	288.1	0.63	0.84
5 mph Target Vehicle	382.7	315.3	0.64	0.85
5 mph Target Vehicle	386.0	329.5	0.62	0.83
5 mph Target Vehicle	390.6	359.8	0.58	0.78
10 mph Target Vehicle	40.3	15.4	0.15	0.19
10 mph Target Vehicle	80.7	44.7	0.20	0.27
10 mph Target Vehicle	111.5	88.8	0.19	0.26
10 mph Target Vehicle	139.9	118.5	0.23	0.30
10 mph Target Vehicle	164.7	132.6	0.28	0.38
10 mph Target Vehicle	198.9	147.0	0.37	0.50
10 mph Target Vehicle	248.9	182.8	0.47	0.62
10 mph Target Vehicle	264.9	209.3	0.46	0.62
10 mph Target Vehicle	271.3	225.3	0.45	0.60
10 mph Target Vehicle	279.3	242.1	0.44	0.59
10 mph Target Vehicle	296.9	267.6	0.45	0.61
10 mph Target Vehicle	322.2	288.5	0.50	0.66
10 mph Target Vehicle	370.5	315.7	0.60	0.80
10 mph Target Vehicle	375.4	328.0	0.59	0.79
10 mph Target Vehicle	382.2	363.4	0.55	0.74
15 mph Target Vehicle	20.7	18.9	0.03	0.04
15 mph Target Vehicle	63.3	48.3	0.11	0.15
15 mph Target Vehicle	73.8	91.1	0.08	0.11
15 mph Target Vehicle	87.9	123.9	0.09	0.11
15 mph Target Vehicle	97.4	136.4	0.10	0.13
15 mph Target Vehicle	104.4	148.2	0.10	0.14
15 mph Target Vehicle	202.8	183.4	0.31	0.41
15 mph Target Vehicle	231.8	209.7	0.35	0.47
15 mph Target Vehicle	241.6	226.5	0.36	0.47
15 mph Target Vehicle	233.7	242.9	0.31	0.41
15 mph Target Vehicle	249.8	268.3	0.32	0.43
15 mph Target Vehicle	263.1	288.1	0.33	0.44
15 mph Target Vehicle	306.0	312.4	0.41	0.55
15 mph Target Vehicle	349.2	327.3	0.51	0.69
15 mph Target Vehicle	365.4	361.9	0.51	0.68
20 mph Target Vehicle	18.8	18.8	0.03	0.03
20 mph Target Vehicle	43.1	47.4	0.05	0.07
20 mph Target Vehicle	54.5	90.3	0.05	0.06
20 mph Target Vehicle	57.7	123.1	0.04	0.05
20 mph Target Vehicle	60.8	132.4	0.04	0.05
20 mph Target Vehicle	72.5	148.2	0.05	0.07
20 mph Target Vehicle	163.9	183.8	0.20	0.27
20 mph Target Vehicle	200.9	212.8	0.26	0.35
20 mph Target Vehicle	208.2	222.2	0.27	0.36
20 mph Target Vehicle	214.6	237.9	0.27	0.36
20 mph Target Vehicle	231.9	271.6	0.27	0.36
20 mph Target Vehicle	248.8	293.2	0.29	0.39
20 mph Target Vehicle	294.7	315.5	0.38	0.51
20 mph Target Vehicle	332.2	333.5	0.46	0.61
20 mph Target Vehicle	344.6	360.3	0.45	0.61

Medium Vehicle (1998 Honda Accord): Roadway Friction Factor, f = 0.75

Specialized Test Feature	Rotational Velocity at Separation, ω (°/sec)	Total Rotational Displacement, θ (°)	Rotational Friction Factor, f_r	Normalized Friction Factor, ξ
25 mph Target Vehicle	0.1	15.4	0.00	0.00
25 mph Target Vehicle	20.4	46.1	0.01	0.02
25 mph Target Vehicle	24.3	93.1	0.01	0.01
25 mph Target Vehicle	35.4	120.5	0.01	0.02
25 mph Target Vehicle	31.3	131.6	0.01	0.01
25 mph Target Vehicle	48.5	153.7	0.02	0.03
25 mph Target Vehicle	95.3	176.9	0.07	0.09
25 mph Target Vehicle	161.6	210.8	0.17	0.23
25 mph Target Vehicle	172.4	227.9	0.18	0.24
25 mph Target Vehicle	175.6	239.1	0.18	0.24
25 mph Target Vehicle	185.5	272.2	0.17	0.23
25 mph Target Vehicle	194.4	293.9	0.18	0.24
25 mph Target Vehicle	206.9	311.8	0.19	0.25
25 mph Target Vehicle	243.0	329.2	0.25	0.33
25 mph Target Vehicle	296.5	358.6	0.34	0.45
25 mph Target Vehicle	307.2	392.3	0.33	0.44
25 mph Target Vehicle	311.5	425.5	0.31	0.42
25 mph Target Vehicle	314.8	453.7	0.30	0.40
25 mph Target Vehicle	329.9	503.8	0.30	0.40
25 mph Target Vehicle	367.2	526.1	0.35	0.47
30 mph Target Vehicle	0.1	15.3	0.00	0.00
30 mph Target Vehicle	0.1	47.3	0.00	0.00
30 mph Target Vehicle	0.1	88.1	0.00	0.00
30 mph Target Vehicle	0.1	120.0	0.00	0.00
30 mph Target Vehicle	0.1	135.0	0.00	0.00
30 mph Target Vehicle	45.7	167.8	0.02	0.02
30 mph Target Vehicle	79.6	179.2	0.05	0.07
30 mph Target Vehicle	132.5	211.2	0.11	0.15
30 mph Target Vehicle	137.3	224.7	0.12	0.15
30 mph Target Vehicle	140.3	240.6	0.11	0.15
30 mph Target Vehicle	140.0	271.0	0.10	0.13
30 mph Target Vehicle	145.9	290.2	0.10	0.13
30 mph Target Vehicle	155.6	314.7	0.11	0.14
30 mph Target Vehicle	171.4	328.8	0.12	0.16
30 mph Target Vehicle	238.6	362.2	0.22	0.29
30 mph Target Vehicle	248.0	392.2	0.22	0.29
30 mph Target Vehicle	255.4	427.1	0.21	0.28
30 mph Target Vehicle	261.0	450.9	0.21	0.28
30 mph Target Vehicle	271.6	507.0	0.20	0.27
30 mph Target Vehicle	300.4	531.5	0.23	0.31
4 locked wheels	60.1	15.7	0.32	0.42
4 locked wheels	110.4	48.6	0.35	0.46
4 locked wheels	151.7	92.0	0.35	0.46
4 locked wheels	181.1	120.3	0.38	0.50
4 locked wheels	201.0	132.7	0.42	0.56
4 locked wheels	245.5	153.3	0.54	0.72
4 locked wheels	269.8	177.1	0.57	0.76
4 locked wheels	298.5	211.6	0.58	0.77
4 locked wheels	309.1	225.5	0.58	0.78
4 locked wheels	321.1	242.4	0.59	0.78
4 locked wheels	341.2	267.5	0.60	0.80
4 locked wheels	360.5	293.8	0.61	0.81
4 locked wheels	374.8	318.1	0.61	0.81
4 locked wheels	379.4	329.3	0.60	0.80
4 locked wheels	393.0	362.7	0.59	0.78
1 locked wheel	61.3	17.0	0.30	0.41
1 locked wheel	101.3	42.8	0.33	0.44
1 locked wheel	161.9	89.5	0.40	0.54
1 locked wheel	206.2	116.3	0.50	0.67
1 locked wheel	237.8	133.3	0.59	0.78
1 locked wheel	253.5	149.5	0.59	0.79
1 locked wheel	270.5	177.3	0.57	0.76
1 locked wheel	290.4	212.6	0.55	0.73
1 locked wheel	299.1	226.8	0.54	0.73
1 locked wheel	308.1	239.4	0.55	0.73

1 locked wheel	336.1	269.2	0.58	0.77
1 locked wheel	353.5	289.1	0.60	0.80
1 locked wheel	363.2	315.1	0.58	0.77
1 locked wheel	367.5	331.5	0.56	0.75
1 locked wheel	373.6	363.1	0.53	0.71
Impact at front end	59.8	16.7	0.30	0.39
Impact at front end	107.6	46.2	0.35	0.46
Impact at front end	191.0	87.1	0.58	0.77
Impact at front end	227.8	118.6	0.60	0.80
Impact at front end	235.8	136.1	0.56	0.75
Impact at front end	238.7	148.5	0.53	0.71
Impact at front end	244.5	181.4	0.45	0.61
Impact at front end	250.3	212.3	0.41	0.54
Impact at front end	251.9	223.0	0.39	0.52
Impact at front end	255.6	240.7	0.37	0.50
Impact at front end	271.0	273.9	0.37	0.49
Impact at front end	282.6	287.7	0.38	0.51
Impact at front end	313.3	314.3	0.43	0.57
Impact at front end	319.5	327.2	0.43	0.57
Impact at front end	331.8	360.3	0.42	0.56

Large Vehicle (1998 Ford Expedition): Roadway Friction Factor, f = 0.75

Specialized Test Feature	Rotational Velocity at Separation, ω (°/sec)	Total Rotational Displacement, θ (°)	Rotational Friction Factor, f_r	Normalized Friction Factor, ξ
Impact at front end	58.9	17.4	0.28	0.37
Impact at front end	97.4	42.4	0.31	0.41
Impact at front end	180.2	92.8	0.48	0.64
Impact at front end	212.5	118.4	0.53	0.70
Impact at front end	222.7	138.7	0.49	0.66
Impact at front end	226.8	152.0	0.47	0.62
Impact at front end	235.2	181.7	0.42	0.56
Impact at front end	238.9	212.1	0.37	0.49
Impact at front end	244.6	227.9	0.36	0.48
Impact at front end	249.8	243.3	0.35	0.47
Impact at front end	270.6	268.3	0.38	0.50
Impact at front end	301.5	290.5	0.43	0.58
Impact at front end	313.6	316.9	0.43	0.57
Impact at front end	318.0	332.1	0.42	0.56
Impact at front end	324.7	363.4	0.40	0.53

APPENDIX C

New Lorentz, curve fit formulas.

Large target vehicle curve fit from figure 1.

$$\xi = \frac{19750}{\pi(4(\theta - 123.2)^2 + 14010)} + \frac{1390}{\pi(4(\theta - 302.8)^2 + 3426)} + \frac{857000}{\pi(4(\theta - 423.6)^2 + 454700)}$$

Medium target vehicle curve fit from figure 2.

$$\xi = \frac{58720}{\pi(4(\theta - 141.8)^2 + 37660)} + \frac{4841}{\pi(4(\theta - 295.3)^2 + 5987)} + \frac{234700}{\pi(4(\theta - 420.9)^2 + 126100)}$$

Small target vehicle curve fit from figure 3.

$$\xi = \frac{13550}{\pi(4(\theta - 139.6)^2 + 10800)} + \frac{1457}{\pi(4(\theta - 303.5)^2 + 2330)} + \frac{682700}{\pi(4(\theta - 430.7)^2 + 314100)}$$

Combined target vehicle curve fit from figure 4.

$$\xi = \frac{29150}{\pi(4(\theta - 134.9)^2 + 20700)} + \frac{2981}{\pi(4(\theta - 300.8)^2 + 4763)} + \frac{585600}{\pi(4(\theta - 449.3)^2 + 290100)}$$

APPENDIX D

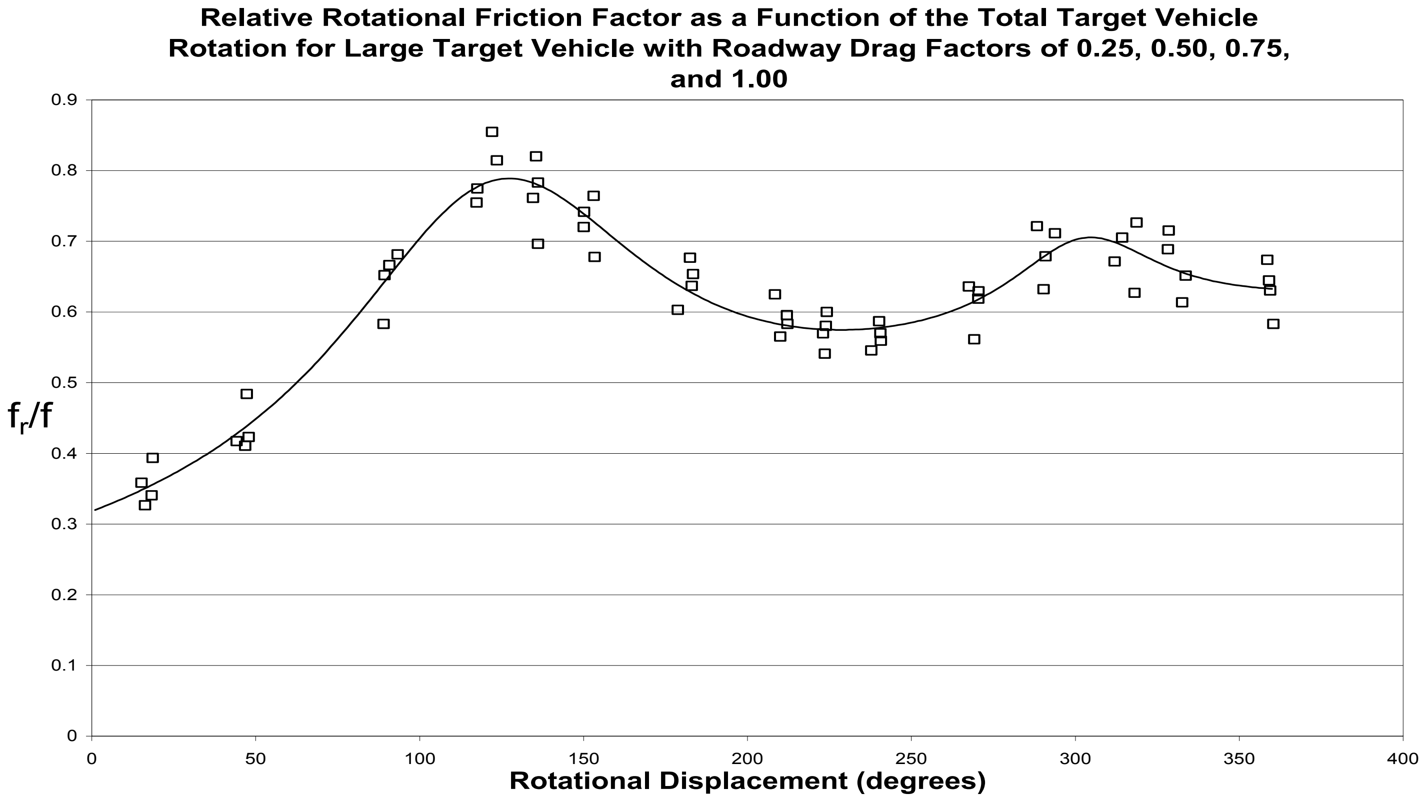

Figure 1

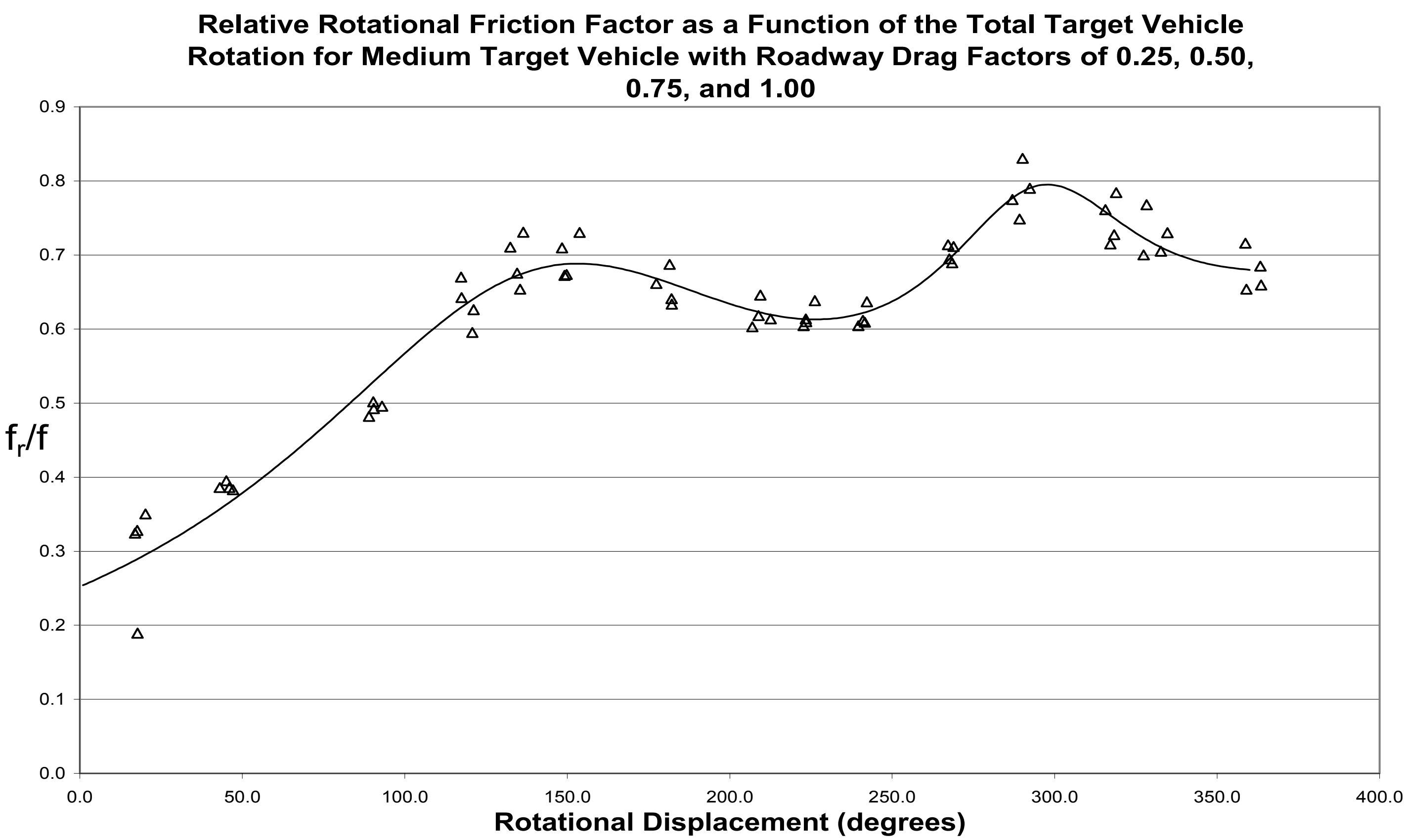

Figure 2

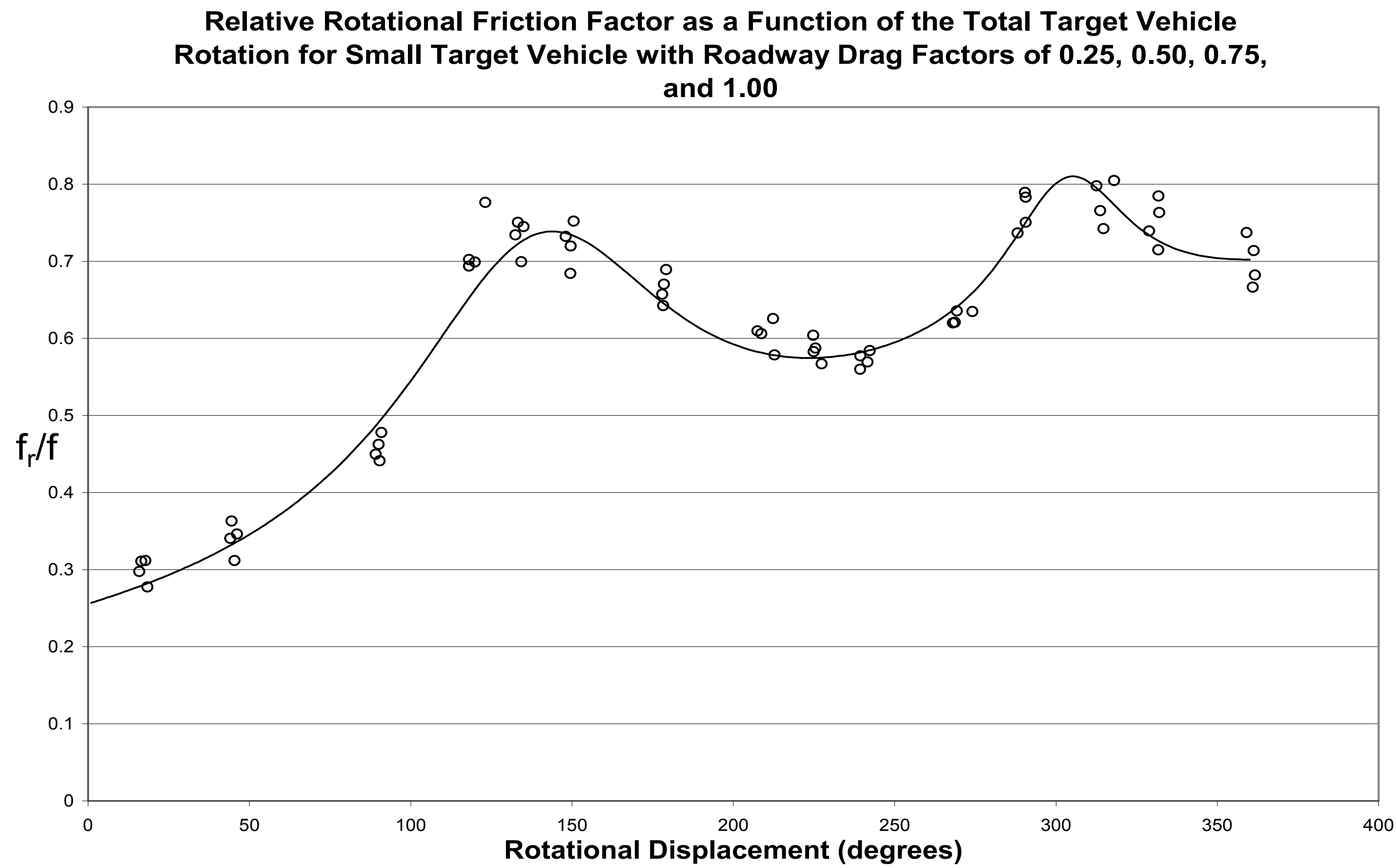

Figure 3

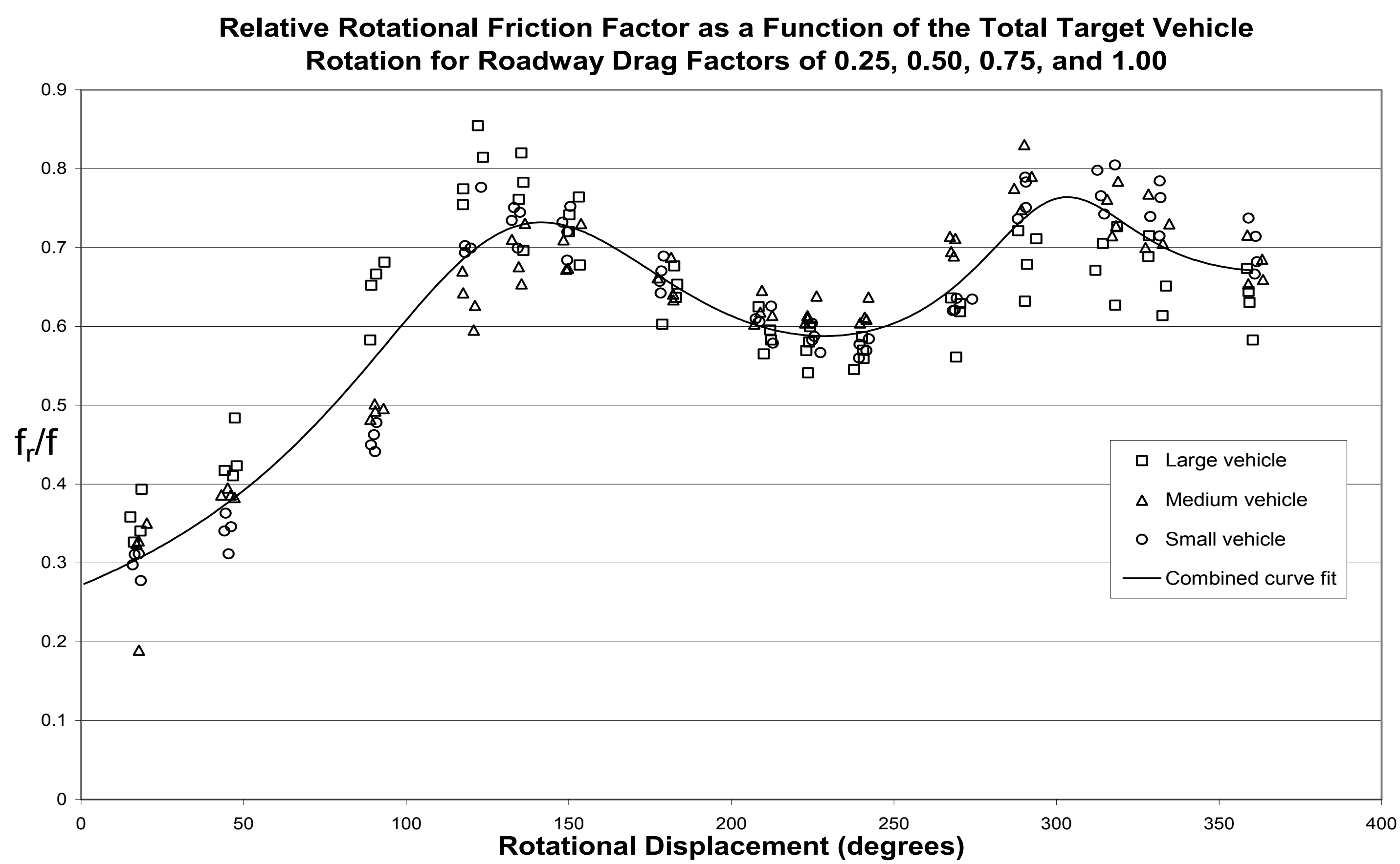

Figure 4

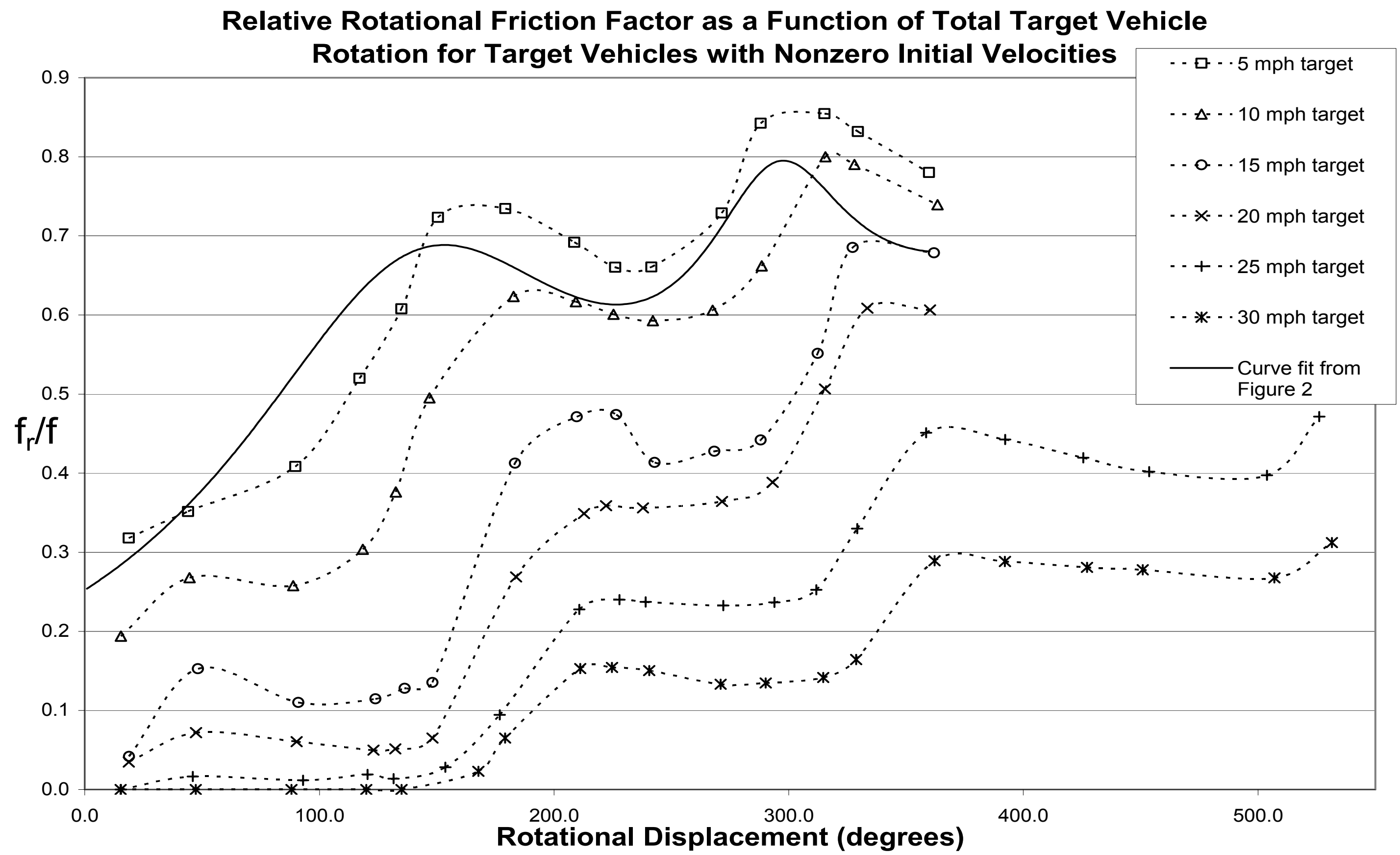

Figure 5

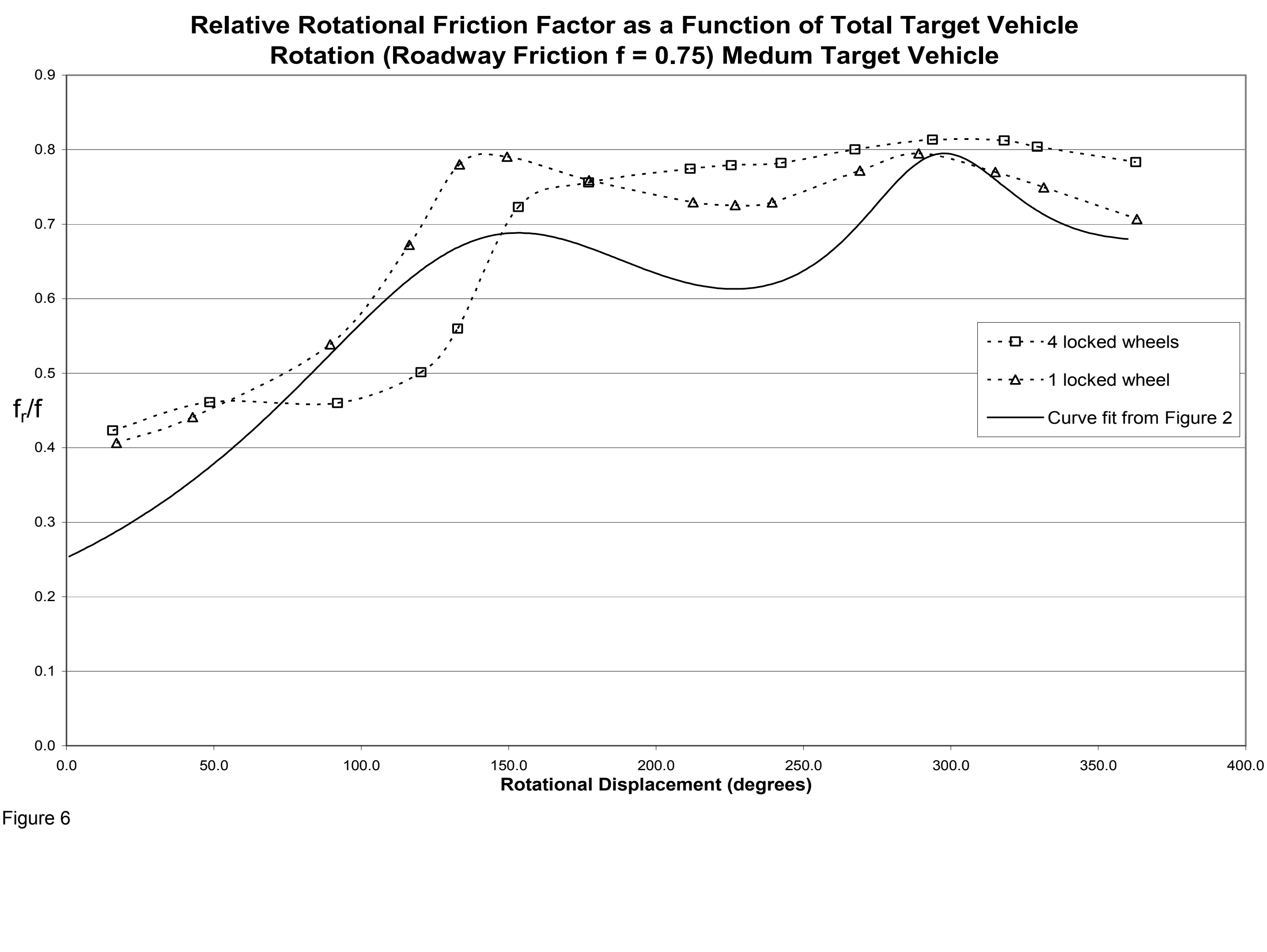

Figure 6

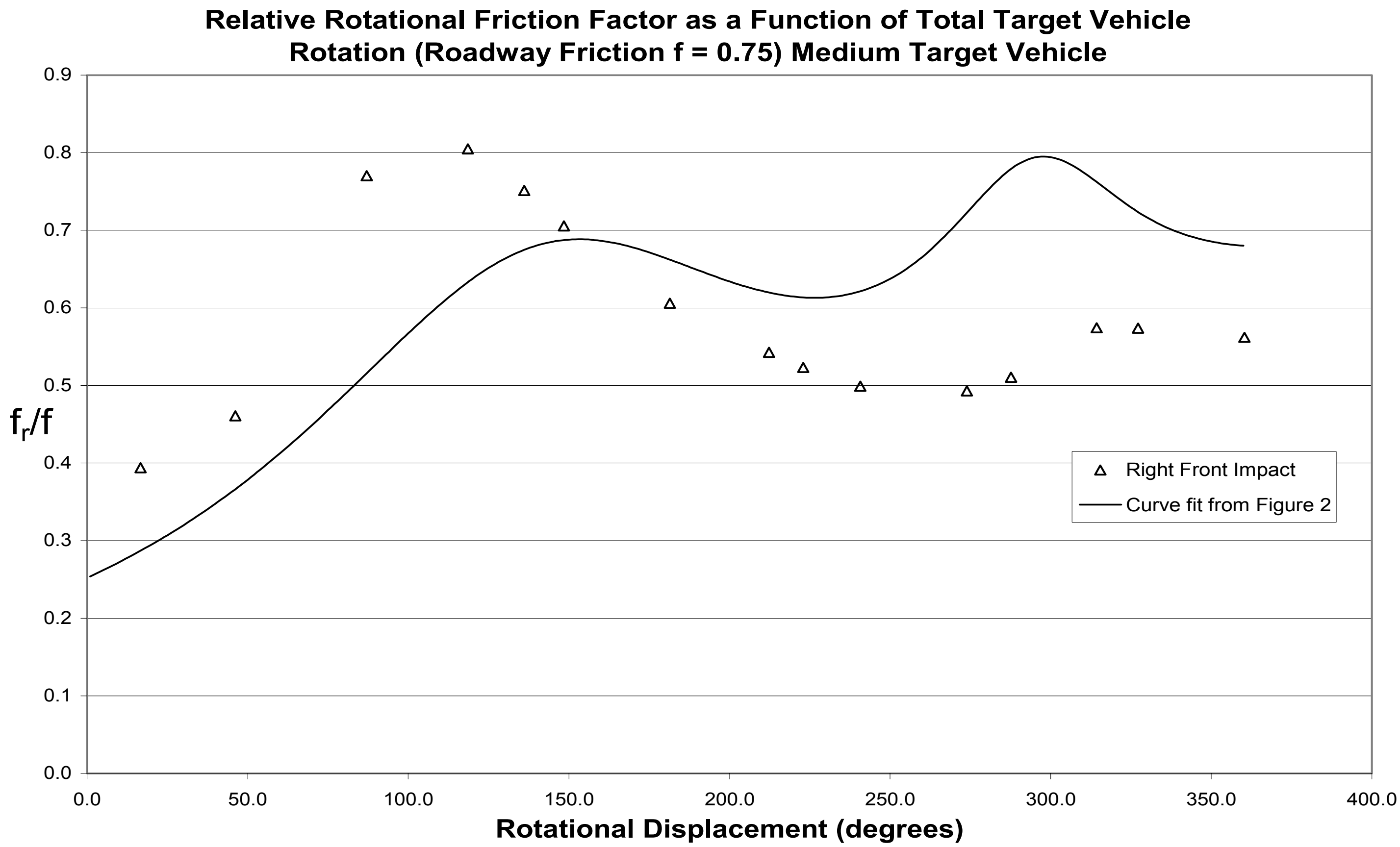

Figure 7

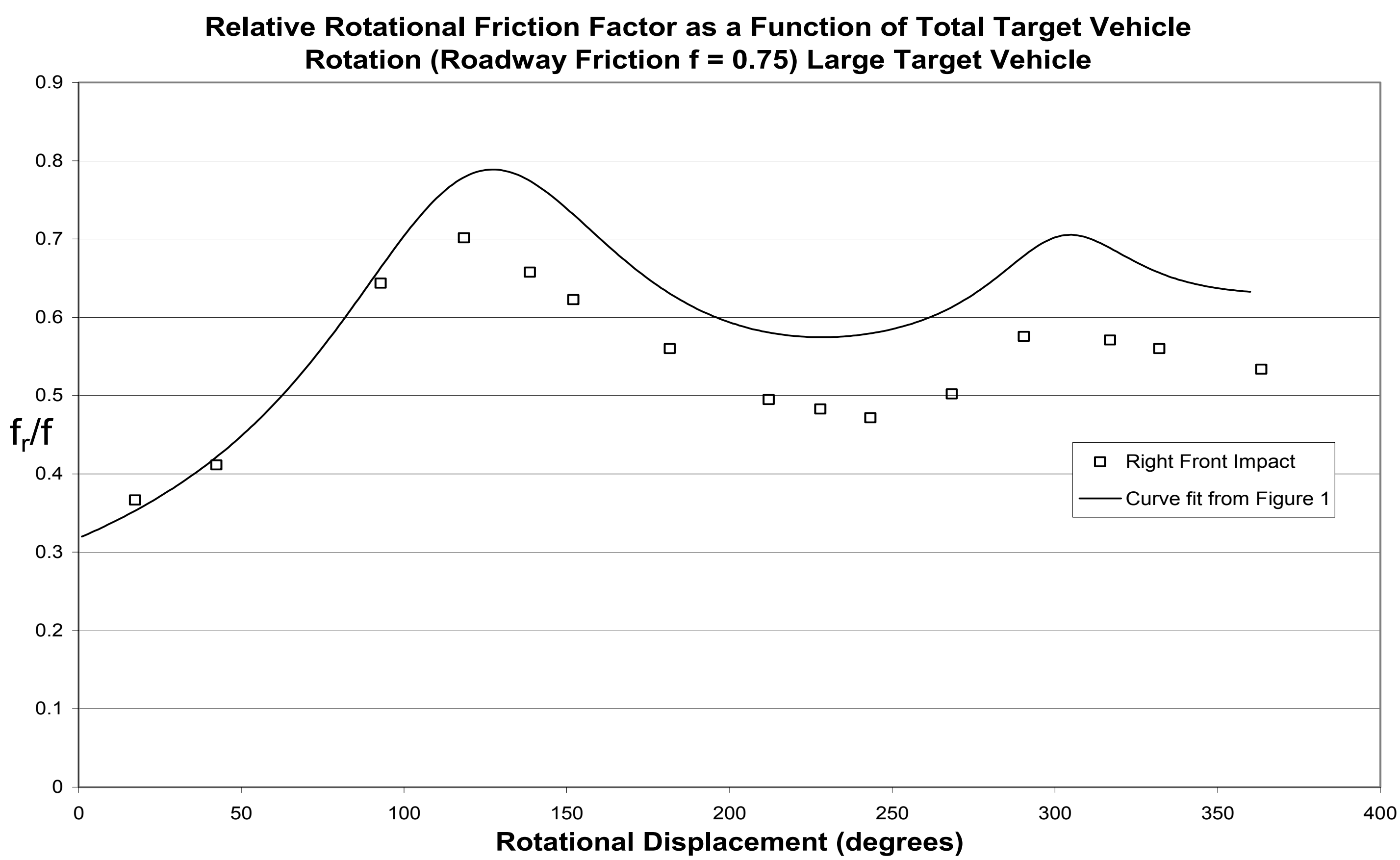

Figure 8